Available online at www.sciencedirect.com
SCIENCE DIRECT®
C. R. Chimie 8 (2005) 1766–1773
COMPTES RENDUS CHIMIE
http://france.elsevier.com/direct/CRAS2C/

Full paper / Mémoire

Synthesis and crystal structure of $2[(Ta_6Cl_{12})Cl_3(n\text{-BuCN})_3]\cdot[(Ta_6Cl_{12})Cl_4(n\text{-BuCN})_2]\cdot n\text{-BuCN}$. The first cluster compound containing $[Ta_6Cl_{12}]^{3+}$ and $[Ta_6Cl_{12}]^{4+}$ cores

Pavica Planinić [a,*], Vesna Rastija [b], Berislav Perić [a], Gerald Giester [c], Nevenka Brničević [a,*]

[a] *Division of Material Chemistry, Rudjer Bošković Institute, P.O. Box 180, 10002 Zagreb, Croatia*
[b] *Department of Chemistry, Faculty of Agriculture, The Josip Juraj Strossmayer University, 31001 Osijek, Croatia*
[c] *Institute für Mineralogie und Kristallographie, Universität Wien-Geozentrum, Althanstrasse 14, A-1090 Wien, Austria*

Received 7 September 2004; accepted after revision 17 January 2005

Available online 14 June 2005

Abstract

By partial oxidation of a solution of $(Ta_6Cl_{12})Cl_2\cdot 6$ EtOH in *n*-butyl cyanide (*n*-BuCN) reddish crystals of the title compound were formed. The compound crystallizes in the monoclinic *C*2/*m* space group. The double salt components $[(Ta_6Cl_{12})Cl_3(n\text{-BuCN})_3]$ and $[(Ta_6Cl_{12})Cl_4(n\text{-BuCN})_2]$ are of C_s and C_{2h} symmetry, respectively. The structure consists of layers formed by the intergrown one-dimensional chains of the different cluster components. The crystal structure analysis and UV spectra revealed differently charged cluster entities, namely $[Ta_6Cl_{12}]^{3+}$ and $[Ta_6Cl_{12}]^{4+}$ in $[(Ta_6Cl_{12})Cl_3(n\text{-BuCN})_3]$ and $[(Ta_6Cl_{12})Cl_4(n\text{-BuCN})_2]$, respectively. ***To cite this article: P. Planinić et al., C. R. Chimie 8 (2005)***.
© 2005 Académie des sciences. Published by Elsevier SAS. All rights reserved.

Résumé

Par oxydation partielle de la solution de $(Ta_6Cl_{12})Cl_2\cdot 6$ EtOH dans le cyanure de *n*-butyle (*n*-BuCN), des cristaux rougeâtres du présent composé ont été obtenus. Le nouveau composé cristallise dans le group d'espace monoclinique *C*2/*m*. Les composants du sel double $[(Ta_6Cl_{12})Cl_3(n\text{-BuCN})_3]$ et $[(Ta_6Cl_{12})Cl_4(n\text{-BuCN})_2]$ possèdent la symétrie C_s et C_{2h}, respectivement. La structure consiste en couches formées par imbrication des chaînes unidimensionnelles de constituants divers du cluster. L'analyse structurale et le spectre UV montrent que les entités du cluster $[(Ta_6Cl_{12})Cl_3(n\text{-BuCN})_3]$ et $[(Ta_6Cl_{12})Cl_4(n\text{-BuCN})_2]$ ont des charges différentes, c'est-à-dire $[Ta_6Cl_{12}]^{3+}$ et $[Ta_6Cl_{12}]^{4+}$, respectivement. ***Pour citer cet article : P. Planinić et al., C. R. Chimie 8 (2005)***.
© 2005 Académie des sciences. Published by Elsevier SAS. All rights reserved.

* Corresponding authors.
E-mail addresses: planinic@rudjer.irb.hr (P. Planinić), brnicevi@rudjer.irb.hr (N. Brničević).

1631-0748/$ - see front matter © 2005 Académie des sciences. Published by Elsevier SAS. All rights reserved.
doi:10.1016/j.crci.2005.02.026

Keywords: Hexanuclear tantalum cluster; Differently charged cluster units; Crystal structure; Coordinated *n*-butyl cyanide

Mots clés : Cluster de tantale hexanucléaire ; Entités du cluster de charges différentes ; Structure cristalline ; Cyanure de *n*-butyle coordonné

1. Introduction

So far, in our laboratory several compounds containing cation–anion cluster pairs with differently charged cluster units have been prepared [1]. The first examples were heteronuclear clusters $[M_6X_{12}(EtOH)_6]$-$[(Mo_6Cl_8)Cl_4X_2]\cdot n$ EtOH$\cdot m$ Et_2O (M = Nb, Ta; X = Cl, Br) containing $[M_6X_{12}]^{2+}$ in the cation and $[Mo_6Cl_8]^{4+}$ in the anion [2]. Later on a homonuclear member of the series having the composition $[Ta_6Cl_{12}(PrCN)_6]$-$[(Ta_6Cl_{12})Cl_6]\cdot 2$ PrCN with $[Ta_6Cl_{12}]^{2+}$ in the cluster cation and $[Ta_6Cl_{12}]^{4+}$ in the cluster anion was prepared [3]. The triclinic phases $[Ta_6Br_{12}(H_2O)_6]X_2\cdot$ *trans*-$[Ta_6Br_{12}(OH)_4(H_2O)_2]\cdot 18\ H_2O$ (X = Cl, Br, NO_3) with the coexistence of $[Ta_6Br_{12}]^{2+}$ in $[Ta_6Br_{12}$-$(H_2O)_6]^{2+}$ and $[Ta_6Br_{12}]^{4+}$ in *trans*-$[Ta_6Br_{12}(OH)_4$-$(H_2O)_2]$ were also obtained [4]. Having initially examined the reactions of $[M_6X_{12}]^{2+}$ with several alkyl cyanides [3,5,6] it was reasonable to extend the reactions to *n*-BuCN.

Using $(Ta_6Cl_{12})Cl_2\cdot$6EtOH as a suitable precursor in the reactions with *n*-BuCN we have isolated the double salt $2[(Ta_6Cl_{12})Cl_3(n\text{-BuCN})_3]\cdot[(Ta_6Cl_{12})Cl_4(n$-$BuCN)_2]\cdot n$-BuCN, consisting of differently charged cluster entities: $[Ta_6Cl_{12}]^{3+}$ in $[(Ta_6Cl_{12})Cl_3(n\text{-BuCN})_3]$ (**A**) and $[Ta_6Cl_{12}]^{4+}$ in $[(Ta_6Cl_{12})Cl_4(n\text{-BuCN})_2]$ (**B**). To our knowledge this is the first structurally characterized substance with coordinated *n*-BuCN.

2. Experimental section

2.1. Materials

All manipulations were performed with the use of an inert atmosphere dry-box, high vacuum manifold or Schlenk techniques. The starting cluster $(Ta_6Cl_{12})Cl_2\cdot$ 6 EtOH was prepared from $[(Ta_6Cl_{12})Cl_2(H_2O)_4]\cdot 4\ H_2O$ by a repeated process of dissolution in dry ethanol following evaporation of the solution in high vacuum to form the ethanol coordinated cluster (usually 3–5 distillation/evaporation cycles) as described earlier [7]. Absolute ethanol (p. a. grade, Kemika) was dried over sodium ethoxide, formed by dissolving metallic sodium in ethanol, followed by distillation in high vacuum onto activated 3-Å molecular sieves. Butyl cyanide (valeronitrile, *n*-pentanenitrile, $CH_3(CH_2)_3CN$) (Aldrich, 99.5%) was treated with activated 3 Å molecular sieves before use.

2.2. Physical measurements

Elemental analyses for carbon, hydrogen and nitrogen were obtained using a Perkin Elmer Model 2400 microanalytical analyzer.

The infrared spectrum (4000–200 cm^{-1}) was obtained as a KBr pellet on a Bomem MB-102 Fourier transform infrared spectrometer. The solid state electronic spectrum (200–2000 nm) of a KBr pelletized sample was recorded using an UV/VIS/NIR Varian Cary-5 spectrometer with a KBr pellet as the reference.

2.3. Synthesis of 2 $[(Ta_6Cl_{12})Cl_3$(n-*BuCN*$)_3]\cdot$ $[(Ta_6Cl_{12})Cl_4$(n-*BuCN*$)_2]\cdot$n-*BuCN*

In a dry-box the cluster $(Ta_6\ Cl_{12})Cl_2\cdot$6 EtOH (0.300 g; 0.162 mmol) was transferred into a 100 ml Schlenk flask and *n*-butyl cyanide (10 ml) was added. In the closed Schlenk flask the suspension was stirred magnetically at room temperature and atmospheric pressure. After a 2-h stirring the cluster precursor was completely dissolved. The color of the solution was emerald green. Then, the flask was opened and the clear solution was exposed to the air atmosphere for a period of 3–5 min, then closed and left for several weeks at room temperature. During this period the color of the solution was slowly changing to olive green and finally to dark red. Simultaneously with the changes in the color of the solution the formation of the white gelly-like precipitate of $Ta(OH)_5\cdot n\ H_2O$ was found as a result of the decomposition of a significant number of cluster entities. The process is exactly the same as that observed by the formation of $[Ta_6Cl_{12}(PrCN)_6][(Ta_6Cl_{12})Cl_6]\cdot$ 2 PrCN [3]. Parallel to the cluster decomposition process, dark-red single crystals of the title compound were grown over the walls of the reaction flask. The reaction

was reproducible with the yield of 6–8% for crystals picked up from the walls of the flask.

Anal. Calc. for $C_{45}H_{81}Cl_{46}N_9Ta_{18}$: C, 9.59; H, 1.45; N, 2.24; Found: C, 9.71; H, 1.56; N, 2.14%. IR data (KBr, cm^{-1}): 2960 s, 2935 s, 2873 m, 2289 s, 2250 sh, 1460 m, 1407 m, 1320 w, 1108 w, 329 vs. UV/VIS/NIR (KBr, nm): 216 sh, 234, 351, 422 sh, 768, 805, 887, 954, 1317.

2.4. Structure analysis and refinement

An air-sensitive dark-red crystal of the title compound with approximate dimensions 0.12 × 0.12 × 0.06 mm was selected and attached to the top of a glass capillary. The crystal was mounted under a stream of cold nitrogen at 200 (3) K on the goniometer head of the Nonius Kappa CCD diffractometer. The details of the data collection and structure determination are given in Table 1.

The primitive unit cell parameters, obtained from all measured reflections, were transformed and finally refined according to the *C*-centered monoclinic lattice type. The Laue symmetry checked on the collected data was compatible with the 2/*m* group. The data was corrected for absorption by the multi-scan method of the DENZO-SCALEPACK program [8]. Although the analytical absorption correction was also tried, the better value for the R_{init} was obtained by the multi-scan method (0.0663 vs. 0.1137).

The positions of all tantalum and chlorine (bridging) atoms in the **A** and **B** components were obtained by direct methods using SHELXS-97 program [9]. After a few successive difference Fourier maps, calculated by SHELXL-97 [10] three N≡C–C groups (from *n*-BuCN) and three Cl^- ions attached to the terminal ligand positions of the **A** component, as well as two N≡C–C groups and four Cl^- ions attached to the termi-

Table 1
Crystal data and structural refinement

Molecular formula	2 $[(Ta_6Cl_{12})Cl_3(C_4H_9CN)_3]\cdot[(Ta_6Cl_{12})Cl_4(C_4H_9CN)_2]\cdot C_4H_9CN$
Molecular weight	5635.99
Crystal system	Monoclinic
Space group	*C*2/*m* (No. 12)
a (Å)	33.118(7)
b (Å)	13.634(3)
c (Å)	17.129(3)
β (°)	120.32(3)
V (Å^3)	6676(3)
Z	2
d (g cm^{-3})	2.804
F(000)	5020
μ (Mo Kα) (cm^{-1})	15.62
Absorption corrections, transmission factors	Multi-scan; 0.23 min, 0.60 max
Temperature (K)	200(3)
Θ Range (°)	2.37–30.00
hkl Ranges	–46 46; –19 18; –24 24
Reflections measured	18640
Unique data	10105
Reflections observed	6109
Criterion	> 2 *σ*(*I*)
R_{init}/R_σ	0.066/0.075
Refinement type	Fsqd
Parameters refined	250
[a]R/R_w (observed)	0.061/0.163
Weighting scheme	$w = 1/[\sigma^2(F_o^2) + (0.0845\,P)^2 + 18.9622\,P]$ where $P = (F_o^2 + 2F_c^2)/3$
Goodness-of-fit	1.070
Difference peak/hole (e Å^{-3})	5.35/–2.22

[a] $R = \Sigma||F_o| - |F_c||/\Sigma|F_o|$; $R_w = \Sigma[w(|F_o|^2 - |F_c|^2)^2/\Sigma w(|F_o|^2)^2]^{1/2}$.

nal ligand positions of the **B** component were clearly resolved. All these atoms (as well as other atoms obtained by direct methods) were refined using displacement parameters in an anisotropic model. Positions of the remaining carbon atoms from coordinated *n*-BuCN molecules were also found from subsequent difference Fourier syntheses. Due to the greater conformational freedom of carbon atoms connected by single C–C bonds in the *n*-BuCN molecules, the displacement parameters for these atoms were found to be much larger than those for the other atoms in the structure, so in the final refinements these parameters were used in the isotropic model. Also, the restraints of single C–C bonds to target a value of 1.5 Å, and of C–C–C angles between single C–C bonds to target a value of 109° were used in the final least-squares refinements of the structure.

By completing the structure determination of the **A** and **B** components, there was still a large solvent accessible area in the unit cell (~1742 $Å^3$, i.e. 1/4 of the volume of the unit cell). The difference Fourier maps did not reveal any recognizable molecule in this region (the first nine peaks were located in the vicinity of tantalum atoms). Since the IR spectrum did not indicate any presence of EtOH, it was assumed that the solvent accessible area is disorderly occupied by certain number of *n*-BuCN molecules. To take into account the electron density of the solvent accessible area in the crystal structure, the SQUEEZE procedure in the PLATON program was used [11–14]. In such a way, the final least-square refinements with SHELXL [10] were performed without any atoms located in the solvent region. The SQUEEZE procedure was applied to calculate the overall number of the electrons in the solvent accessible area. The result of calculation indicated 109 electrons. This number roughly corresponds to two additional *n*-BuCN molecules in the unit cell. Based on these calculations, the chemical formula of the title compound was obtained and one additional *n*-BuCN molecule was included in the chemical formula weight, crystal density, *F*(0,0,0) and linear absorption coefficient. Final F_o/F_c Tables were calculated with the PLATON program [11], including electron density in the solvent accessible area.

Also, it should be mentioned that the **A** and **B** components are located at the positions of the *m* and 2/*m* symmetries, according to the presented model in the space group *C*2/*m*. To release these symmetry constraints, the structure was also refined in the subgroups of *C*2/*m* (*C*2, *Cm*, $P\bar{1}$ and *P*1). The refinements in the lower symmetry space groups did not show any improvements of the structural model of the title compound, the highest peaks from difference Fourier maps being always located in the vicinity of the tantalum atoms.

3. Results and discussion

The aliphatic nitriles, *n*-RCN, were found to be suitable solvents for the preparation of clear solutions of $[Ta_6Cl_{12}]^{2+}$ cluster. In a closed Schlenk flask these solutions are stable at room temperature and inert atmosphere. If exposed to air oxygen for a short period of time (up to 5 min) partial oxidation of some $[Ta_6Cl_{12}]^{2+}$ to $[Ta_6Cl_{12}]^{3+}$ and/or $[Ta_6Cl_{12}]^{4+}$ units (having 16, 15 and 14 electrons for Ta–Ta bonding, respectively) takes place. Parallel to this process the decomposition of certain number of cluster entities to $Ta(OH)_5{\cdot}n\ H_2O$ also occurs. The slow oxidation process of the starting cluster allows the coexistence of several $[Ta_6Cl_{12}]^{n+}$ (n = 2, 3, 4) species in the solution. This seems to be convenient for the formation of solid state phases with differently charged cluster entities.

The position of the absorption bands in the IR spectrum of the title compound is given in the Experimental part. The regions of the spectrum 3500–3000, 1600–1650 and 1050–1000 cm^{-1} are free of absorptions confirming the absence of any water or ethanol molecules in the compound. The strong absorption band at 2289 cm^{-1} originates from the CN stretching vibrations of *n*-BuCN. It is shifted to higher wave numbers for 41 cm^{-1} in comparison to its position in the free ligand (2248 cm^{-1}). This is in accord with the nitrile molecules being coordinated through the σ-bonded nitrogen atom [15,16]. The CN stretching absorption band from free *n*-BuCN molecule is not resolved and cannot be exactly identified in the IR spectrum of the title compound. The situation is analogous to that for the $[Ta_6Cl_{12}(PrCN)_6][(Ta_6Cl_{12})Cl_6]{\cdot}2$ PrCN cluster [3]. Very probably, this absorption is causing broadening (like a shoulder) of the upper part of the CN stretching absorption band from coordinated *n*-BuCN on the side of lower wave numbers (~2250 cm^{-1}), where the absorption of CN group from free *n*-BuCN molecule is expected. The strongest absorption band in the spec-

trum present at 329 cm^{-1} originates from the Ta–Cl (μ-Cl) stretching vibrations.

A complex electronic spectrum in the visible region (see Section 2) shows the superposition of characteristic bands of the $[Ta_6Cl_{12}]^{3+}$ and $[Ta_6Cl_{12}]^{4+}$ units [17–19] and is in agreement with the results of the X-ray structure analysis. The presence of paramagnetic $[Ta_6Cl_{12}]^{3+}$ cluster unit is also indicated by some preliminary data from EPR spectra and magnetic susceptibility measurements that will be discussed separately.

3.1. Crystal structure

The title compound is a double salt consisting of three neutral octahedral cluster entities: two $[(Ta_6Cl_{12})Cl_3(n\text{-BuCN})_3]$ and one $[(Ta_6Cl_{12})Cl_4(n\text{-BuCN})_2]$. The ORTEP-3 drawings [20] of these entities are shown in Fig. 1. Six terminal octahedral coordination sites in the **A** components are occupied by 3 Cl^- ions and 3 *n*-BuCN molecules. Unexpectedly, all Cl^- are in *cis* position as are the *n*-BuCN ligands. In the **B** component, the terminal coordination positions are occupied by 4 Cl^- ions in equatorial positions and by 2 *n*-BuCN molecules in apical *trans* positions. The **A** components have C_s symmetry with a mirror plane passing through the Ta2, Ta4, Cl14, Cl32 and Cl4 atoms. The *n*-BuCN molecule bonded to the Ta2 atom lies completely in this symmetry plane (Fig. 1a). Such molecular symmetry is in accordance with crystallographic positions of the **A** components in the structure (sites with *m* symmetry). The **B** components are located on the crystallographic positions of higher symmetry (2/*m*). Accordingly, the molecular symmetry of the **B** components belongs to the C_{2h} group. The mirror plane in the **B** component passes through the Ta5, $Ta5^{ii}$, Cl62 and $Cl62^{ii}$ atoms [symmetry code: (*ii*) –*x*, *y*, –*z*] and through the both coordinated *n*-BuCN molecules (Fig. 2b). A second order rotation axis passes through the Cl12 and $Cl12^{i}$ atoms [symmetry code: (*i*) *x*, –*y*, *z*]. According to the difference Fourier synthesis, the terminal carbon atom of the coordinated *n*-BuCN molecules in the **B** component is located outside of the

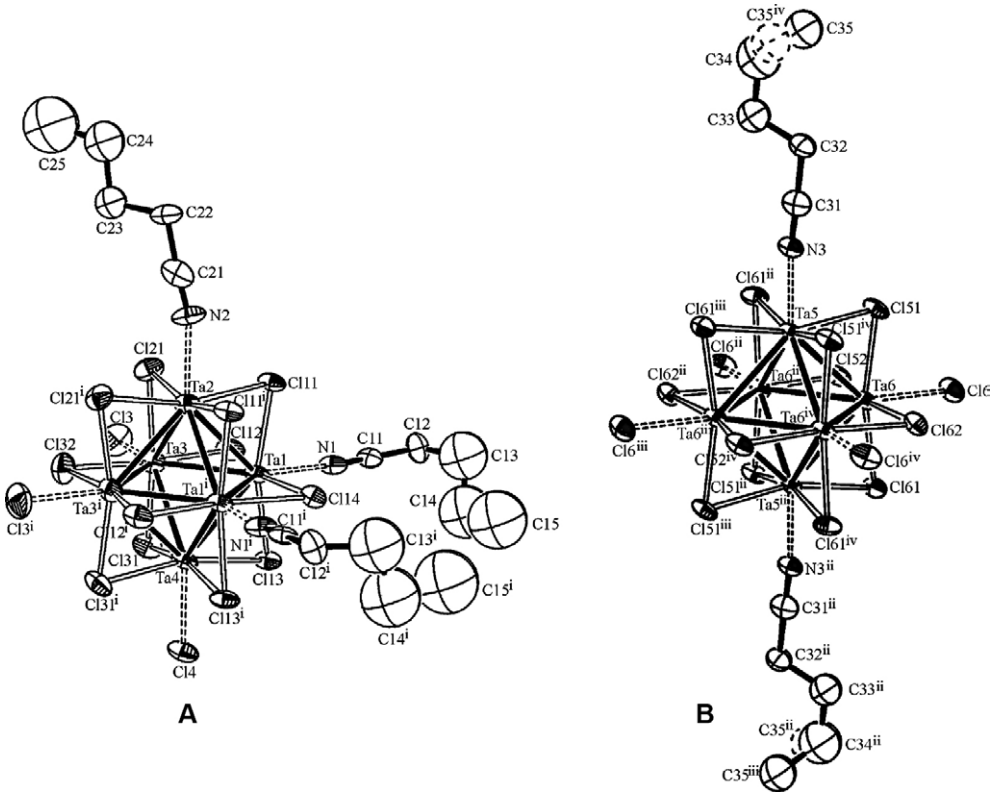

Fig. 1. Molecular structures of **A** (left) and **B** (right) components. The C35 atom is located disorderly at two different positions. One position is shown solid, the other is shown dashed. Symmetry codes are given in Tables 2 and 3.

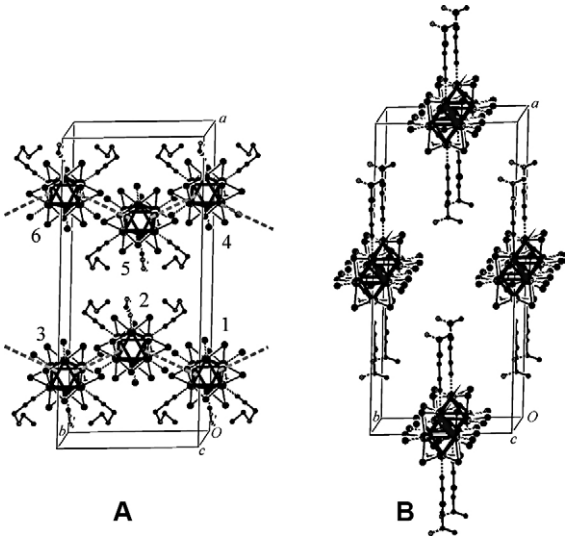

Fig. 2. Crystal packing of **A** (left) and **B** (right) components in the unit cell. One-dimensional chains of **A** components are denoted as dashed lines.

mirror plane, and is disordered over two symmetry equivalent sites: C35 and C35^{iv} [symmetry code: (*iv*) *x*, 1 – *y*, *z*]. Thus, the site occupation factor for the C35 atom is 0.5. Also, one of the major consequences of the different crystallographic positions of the **A** and **B** components in the structure, is a double amount of the **A** component in the formula unit of the compound.

The main difference between the **A** and **B** components is the charge of the cluster units. The **A** components contain $[Ta_6Cl_{12}]^{3+}$, while **B** contains $[Ta_6Cl_{12}]^{4+}$. This is evident from the number of Cl^- ions in terminal octahedral coordination sites and also from the analysis of bond lengths (Table 2). The Ta–Ta bond lengths in the **A** components are in the range 2.8950(9)–2.957(1) Å (average 2.9209 Å) and indicate a slight distortion of the Ta_6 octahedra, but are still in the range of distances found for other $[Ta_6Cl_{12}]^{3+}$ compounds, like $CsPb[(Ta_6Cl_{12})Cl_6]$ (2.925 Å) [21] and $[(Ta_6Cl_{12})Cl(H_2O)_5][HgBr_4]\cdot 9\,H_2O$ (2.911 Å) [22]. The Ta–Ta bond lengths in **B** are in the range 2.9202(9)–2.9640(9) Å (average 2.9348 Å). As expected, in this component the Ta–Ta bond lengths are on the average 0.0139 Å longer than in the **A** components containing $[Ta_6Cl_{12}]^{3+}$ unit. Namely, lengthening of the M–M bonds with an increase of charge on the cluster unit is usually observed within the $[M_6X_{12}]^{n+}$ (M = Nb, Ta; X = Cl, Br; *n* = 2, 3, 4) clusters and this fact also confirms the presence of $[Ta_6Cl_{12}]^{4+}$ in the **B** component

Table 2
Bond lengths in the title compound (Å)

Ta1–Ta1^{i}	2.8950(9)	C11–C12	1.48(2)
Ta1–Ta2	2.898(1)	C12–C13	1.47(4)
Ta1–Ta3	2.908(1)	C13–C14	1.48(5)
Ta1–Ta4	2.920(1)	C14–C15	1.49(8)
Ta2–Ta3	2.921(1)	C21–C22	1.50(2)
Ta3–Ta3^{i}	2.948(1)	C22–C23	1.50(3)
Ta3–Ta4	2.957(1)	C23–C24	1.53(3)
Ta1–Cl11	2.446(3)	C24–C25	1.50(7)
Ta1–Cl12	2.418(3)	Ta5–Ta6	2.927(1)
Ta1–Cl13	2.435(3)	Ta5–Ta6^{ii}	2.9202(9)
Ta1–Cl14	2.454(4)	Ta6–Ta6^{ii}	2.9504(9)
Ta2–Cl11	2.436(3)	Ta6–Ta6^{iv}	2.9640(9)
Ta2–Cl21	2.444(4)	Ta5–Cl51	2.427(3)
Ta3–Cl12	2.448(3)	Ta5–Cl61^{ii}	2.443(3)
Ta3–Cl21	2.454(3)	Ta6–Cl51	2.446(3)
Ta3–Cl31	2.448(5)	Ta6–Cl52	2.438(2)
Ta3–Cl32	2.426(6)	Ta6–Cl61	2.446(3)
Ta4–Cl13	2.448(3)	Ta6–Cl62	2.447(4)
Ta4–Cl31	2.437(4)	Ta5–N3	2.22(2)
Ta1–N1	2.25(1)	Ta6–Cl6	2.511(3)
Ta2–N2	2.28(2)	N3–C31	1.16(3)
Ta3–Cl3	2.477(6)	C31–C32	1.50(3)
Ta4–Cl4	2.509(5)	C32–C33	1.48(3)
N1–C11	1.09(2)	C33–C34	1.51(5)
N2–C21	1.09(2)	C34–C35	1.46(5)

Symmetry codes: (*i*) *x*, –*y*, *z*; (*ii*) –*x*, *y*, –*z*; (*iii*) –*x*, 1 – *y*, –*z*; (*iv*) *x*, 1 – *y*, *z*.

in comparison to the presence of $[Ta_6Cl_{12}]^{3+}$ in **A**. For the **A** component, the Ta–Cl^{a} (a = outside, terminal) bond lengths are in the range of 2.477(6)–2.509(5) Å. The average value of 2.488 Å is very close to the average value of 2.482 Å found for *cis*-$[(Ta_6Cl_{12})Cl_2(PEt_3)_4][BF_4]\cdot 3\,CH_2Cl_2$ containing $[Ta_6Cl_{12}]^{3+}$ [23]. For the **B** component, the Ta–Cl^{a} bond length is 2.511(3) Å, a value slightly longer than in **A**, but still very close to the mean value of 2.507 Å found for $H_2[(Ta_6Cl_{12})Cl_6]\cdot 6\,H_2O$ containing $[Ta_6Cl_{12}]^{4+}$ unit [24]. The Ta–N bond lengths ranging from 2.25(1) Å to 2.28(2) Å (average 2.26 Å) in **A** are slightly longer than in the **B** component [2.22(2) Å]. This could be the consequence of the *cis* arrangement of *n*-BuCN molecules in the former in comparison to their *trans* position in the latter. These values are comparable to the average value of 2.253 Å found for the Ta–N bond lengths in $[Ta_6Cl_{12}(PrCN)_6][(Ta_6Cl_{12})Cl_6]\cdot 2\,PrCN$ [3]. The mean value of N–C bond lengths of coordinated *n*-BuCN molecules in **A** (1.09 Å) is slightly shorter than those in the **B** constituent [1.16(3) Å], but all these val-

ues are usual for a triple C≡N bond [25]. Bond angles, especially those defined on N atoms show roughly linear arrangement of the Ta atoms and C≡N groups of *n*-BuCN molecules attached to them (Table 3). The largest deviation from 180° is obtained for the Ta2–N2–C21 angle [163(2)°], but its value is still much bigger than the mean values of 131° and 130° found for Ta–O–C angles in $[Ta_6Cl_{12}(C_2H_5OH)_6][(Mo_6Cl_8)Cl_6]\cdot 6\,C_2H_5OH$ [2] and $[Ta_6Cl_{12}(CH_3OH)_6]Br_3$ [26], respectively, with EtOH and MeOH molecules located on the octahedral coordination sites of the corresponding $[Ta_6Cl_{12}]^{n+}$ cluster units. The value of the Ta2–N2–C21 angle in the title compound is much closer to the mean value of 161° found for the Ta–N–C angles in $[Bu_4N]_3[Ta_6Cl_{12}(NCS)_6]\cdot 2\,CH_2Cl_2$, having NCS ligands in terminal octahedral positions of the $[Ta_6Cl_{12}]^{3+}$ cluster [27]. Other values for Ta–N–C angles in the title compound (Table 3) correlate well with the data observed for $[Ta_6Cl_{12}(PrCN)_6][(Ta_6Cl_{12})Cl_6]\cdot 2$ PrCN [3]. Because the first single C–C bond in the alkyl chain of *n*-BuCN molecule is oriented oppositely to the C≡N bond [28], there are no structural reasons for the disorder of the second carbon atoms of *n*-BuCN molecules. Structural analysis in this work confirms this result because these atoms were clearly resolved from the first few difference Fourier syntheses. The linear arrangement of the C–C≡N atoms in *n*-BuCN chains is also evident from the N1–C11–C12, N2–C21–C22 and N3–C31–C32 angles (Table 3). The other carbon atoms in the *n*-BuCN chains can have more different conformations (due to the easier torsion movements along the C–C bonds) and this is reflected as a structural disorder encountered during refinements of the title structure (larger displacement parameters for these atoms). So, in the present work, the crystallographic parameters for these atoms are not well defined, but this is not relevant for the determination of the type and the number of ligand species coordinate at the octahedral ligand positions of $[Ta_6Cl_{12}]$ clusters.

Table 3
Selected bond angles (°)

Ta2–Ta1–Ta4	90.97(4)	<L^i–Ta–L^a(N)>(**A**)	81.08
Ta3–Ta1–Ta1^i	90.52(4)	<L^i–Ta–L^a(N)>(**B**)	80.95
Ta3–Ta2–Ta1^i	90.19(4)	<L^i–Ta–L^a(Cl)>(**A**)	82.4
Ta1–Ta3–Ta3^i	89.48(4)	<L^i–Ta–L^a(Cl)>(**B**)	82.42
Ta2–Ta3–Ta4	89.78(4)	Ta1–N1–C11	175(1)
Ta3–Ta4–Ta1^i	89.07(4)	Ta2–N2–C21	163(2)
Ta6–Ta5–Ta6^{iii}	91.32(4)	Ta5–N3–C31	172(2)
Ta5–Ta6–Ta5^{ii}	88.68(4)	N1–C11–C12	178(2)
Ta6^{ii}–Ta6–Ta6^{iv}	90.00(3)	N2–C21–C22	176(3)
<Ta–L^i–Ta>(**A**)	73.49	N3–C31–C32	178(2)
<Ta–L^i–Ta>(**B**)	73.90		

Symmetry codes: (*i*) *x*, –*y*, *z* ; (*ii*) –*x*, *y*, –*z* ; (*iii*) –*x*, 1–*y*, –*z*; (*iv*) *x*, 1–*y*, *z*.

The crystal packing of the **A** and **B** components in the unit cell is shown in Figs. 2 and 3. The **A** components are located at six positions (labeled from 1 to 6 in Fig. 2a): two of them (2 and 5) belong completely to the unit cell, the remaining four lay on the opposite *ac* faces of the unit cell. The entities 1–3, as well as the entities 4–6 are parts of the one-dimensional chains that extrude along the crystallographic *b* axis. The distance between the centers of the two nearest entities inside a chain is 9.191(2) Å, while the distance between the chains (between the entities 2 and 5 in Fig. 2a) is 16.976(2) Å. The *n*-BuCN ligands are oriented outside of the one-dimensional chains allowing the Cl^- ions in terminal positions to be placed inside the chains. The different roles of the *n*-BuCN and Cl^- ligands in the crystal packing can explain their *cis* arrangement in the **A** components. The **B** components are located in the middles of the *a* and *b* axes (Fig. 2b). Analysis of the neighbors also shows that each unit of the **B** component is surrounded by only two nearest units of the same kind, obtained by translation in positive and negative direction of the crystallographic *b* axis [the distance between two nearest neighbors is 13.634(3) Å]. So, the **B** components also form a kind of one-dimensional chain, separately from the chains of the **A** components.

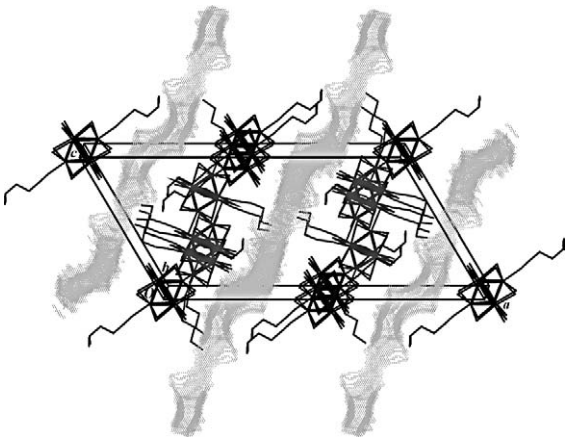

Fig. 3. Intergrowth of **A** (gray) and **B** (black) components in the crystal structure, with the solvent accessible area calculated by PLATON program [11].

In the overall crystal packing, the individual one-dimensional chains of the **A** and **B** components intergrow to form two-dimensional layers parallel with the (2 0 –1) crystallographic planes (Fig. 3). Between these layers there is a solvent accessible area occupied by one *n*-BuCN molecule per formula unit.

4. Conclusion

In aliphatic nitriles it is possible to dissolve the $(M_6Cl_{12})Cl_2{\cdot}6EtOH$ (M = Nb, Ta) clusters. These solutions become suitable media for the preparation of cluster compounds containing two or more units of different charge. So far, the compounds with differently charged cluster entities are obtained for $[Ta_6Cl_{12}]^{n+}$ only. The title compound 2 $[(Ta_6Cl_{12})Cl_3(n\text{-}BuCN)_3]{\cdot}[(Ta_6Cl_{12})Cl_4(n\text{-}BuCN)_2]{\cdot}n\text{-}BuCN$, with the coexistence of $[Ta_6Cl_{12}]^{3+}$ and $[Ta_6Cl_{12}]^{4+}$ units, is unique in the chemistry of hexanuclear clusters of niobium and tantalum. Furthermore, this cluster is the first structurally characterized substance with coordinated *n*-BuCN.

5. Supplementary material

CCDC 248983 contains the supplementary crystallographic data for this paper. These data can be obtained free of charge via www.ccdc.cam.ac.uk/data_request/cif, by emailing data_request@ccdc.cam.ac.uk, or by contacting The Cambridge Crystallographic Data Center, 12, Union Road, Cambridge CB2 1EZ, UK; fax: +44 1223 336 033.

Acknowledgments

This research was supported by the Ministry of Science, Education and Sport of the Republic of Croatia (Grant No. 0098066).

References

[1] N. Brničević, in: P. Braunstein, C. Raithby (Eds.), Metal Clusters in Chemistry, Wiley-WCH Verlag, GmBH, Germany, 1999, p. 1551.
[2] I. Bašic, N. Brničević, U. Beck, A. Simon, R.E. McCarley, Z. Anorg. Allg. Chem. 624 (1998) 725.
[3] N. Brničević, S. Širac, I. Bašic, Z. Zhang, R.E. McCarley, I.A. Guzei, Inorg. Chem. 38 (1999) 4159.
[4] M. Vojnović, N. Brničević, I. Bašic, P. Planinić, G. Giester, Z. Anorg. Allg. Chem. 628 (2002) 401.
[5] S. Širac, R. Trojko, L.J. Marić, R.E. McCarley, O. Tolstikhin, N. Brničević, Croat. Chem. Acta 68 (1995) 905.
[6] P. Planinić, V. Rastija, S. Širac, M. Vojnović, L. Frkanec, N. Brničević, R.E. McCarley, J. Clust. Sci. 13 (2002) 215.
[7] A. Kashta, N. Brničević, R.E. McCarley, Polyhedron 10 (1991) 2031.
[8] Z. Otwinowski, W. Minor, Methods Enzymol. 276 (1997) 307.
[9] G.M. Sheldrick, SHELXS-97, University of Göttingen, Göttingen, Germany, 1997.
[10] G.M. Sheldrick, SHELXL-97, University of Göttingen, Göttingen, Germany, 1997.
[11] A.L. Spek, J. Appl. Crystallogr. 36 (2003) 7.
[12] P. van der Sluis, A.L. Spek, Acta Crystallogr. A46 (1990) 194.
[13] H. Kooijman, A.L. Spek, G.A. van Albada, P. Gamez, J. Reedijk, Acta Crystallogr. C60 (2004) m51.
[14] B. Perić, J. Makarević, M. Jokić, B. Kojić-Prodić, M. Žinić, Acta Crystallogr. C57 (2001) 865.
[15] K. Nakamoto, Infrared and Raman Spectra of Inorganic and Coordination Compounds, Wiley, New York, 1997.
[16] J. Yau, D.M.P. Mingos, J. Chem. Soc., Dalton Trans. (1997) 1103.
[17] B. Spreckelmeyer, Z. Anorg. Allg, Chem. 365 (1969) 225.
[18] P.B. Fleming, R.E. McCarley, Inorg. Chem. 9 (1970) 1347.
[19] C.L. Hussey, R. Quigley, K.R. Seddon, Inorg. Chem. 34 (1995) 370.
[20] L.J. Farrugia, J. Appl. Crystallogr. 30 (1997) 565.
[21] F. Ogliaro, S. Cordier, J.-F. Halet, C. Perrin, J.-Y. Saillard, M. Sergent, Inorg. Chem. 37 (1998) 6199.
[22] N. Brničević, M. Vojnović, S. Antolić, B. Kojić-Prodić, I.D. Desnica-Franković, Solid-State Sci. 1 (1999) 483.
[23] H. Imoto, S. Hayakawa, N. Morita, T. Saito, Inorg. Chem. 29 (1990) 2007.
[24] C.B. Thaxton, A. Jacobson, Inorg. Chem. 10 (1971) 1460.
[25] F.D. Rochon, R. Melanson, E. Thouin, A.L. Beauchamp, C. Bensimon, Can. J. Chem. 74 (1996) 144.
[26] N. Brničević, D. Nöthig-Hus, B. Kojić-Prodić, Z. Ružić-Toroš, Ž. Danilović, R.E. McCarley, Inorg. Chem. 31 (1992) 3924.
[27] N. Prokopuk, V.O. Kennedy, L.C. Stern, D.F. Shriver, Inorg. Chem. 37 (1998) 5001.
[28] R.K. Bohn, J.L. Pardus, J. August, T. Brupbacher, W. Jager, J. Mol. Struct. 413–414 (1997) 293.